Chemosensors **2014**, *2*, 26-40; doi:10.3390/chemosensors2010026

OPEN ACCESS

chemosensors

ISSN 2227-9040

www.mdpi.com/journal/chemosensors

Communication

Selectivity of Chemoresistive Sensors Made of Chemically Functionalized Carbon Nanotube Random Networks for Volatile Organic Compounds (VOC)

Jean-François Feller *, Nicolas Gatt, Bijandra Kumar and Mickaël Castro

Smart Plastics Group, European University of Brittany (UEB), LIMAT^{B}-UBS, 56321 Lorient, France; E-Mails: nicolasgatt@hotmail.fr (N.G.); bijandra@gmail.com (B.K.); mickael.castro@univ-ubs.fr (M.C.)

***** Author to whom correspondence should be addressed; E-Mail: jean-francois.feller@univ-ubs.fr; Tel.: +33-2-9787-4584.

Received: 11 October 2013; in revised form: 17 December 2013 / Accepted: 3 January 2014 / Published: 15 January 2014

Abstract: Different grades of chemically functionalized carbon nanotubes (CNT) have been processed by spraying layer-by-layer (sLbL) to obtain an array of chemoresistive transducers for volatile organic compound (VOC) detection. The sLbL process led to random networks of CNT less conductive, but more sensitive to vapors than filtration under vacuum (bucky papers). Shorter CNT were also found to be more sensitive due to the less entangled and more easily disconnectable conducting networks they are making. Chemical functionalization of the CNT' surface is changing their selectivity towards VOC, which makes it possible to easily discriminate methanol, chloroform and tetrahydrofuran (THF) from toluene vapors after the assembly of CNT transducers into an array to make an e-nose. Interestingly, the amplitude of the CNT transducers' responses can be enhanced by a factor of five (methanol) to 100 (chloroform) by dispersing them into a polymer matrix, such as poly(styrene) (PS), poly(carbonate) (PC) or poly(methyl methacrylate) (PMMA). COOH functionalization of CNT was found to penalize their dispersion in polymers and to decrease the sensors' sensitivity. The resulting conductive polymer nanocomposites (CPCs) not only allow for a more easy tuning of the sensors' selectivity by changing the chemical nature of the matrix, but they also allow them to adjust their sensitivity by changing the average gap between CNT (acting on quantum tunneling in the CNT network). Quantum resistive sensors (QRSs) appear promising for environmental monitoring and anticipated disease diagnostics that are both based on VOC analysis.

Keywords: carbon nanotubes; conductive polymer nanocomposites; e-nose; chemical functionalization; volatile organic compounds; selectivity; sensitivity; detection; spraying layer-by-layer

1. Introduction

Carbon nanotubes (CNT), which were discovered by Lukyanovich *et al.* [1] and further popularized by Iijima [2], have initially attracted a considerable amount of attention, due to their capability to adsorb/desorb small gas molecules, such as hydrogen [3–6] or oxygen [7]. Later on, this interesting feature had been studied for larger molecules, such as volatile organic compounds (VOC) at room temperature [8–12]. Moreover, their unique combination of exceptional electrical conductivity (possibly ballistic) and very high specific surface (resulting from a hollow core and a very large shape factor (L/D)) has made carbon nanotubes one of the most attractive nanomaterials for sensor design [13–19]. This trend is of great interest, as most metal oxide-based sensors operate at several hundred degrees Celsius [20–24]. Carbon nanotube chemoresistive sensors offer significant advantages over conventional metal oxide chemoresistive sensors in terms of the versatility of fabrication (no need for a clean room and low cost), low sensitivity to moisture (no need to operate at a high temperature to get rid of water), high selectivity (several kinds of chemical functionalizations are available, covalent grafting [25–28] or non-covalent bonding [25,29–33]), high sensitivity (due to quantum tunneling conduction [34–39]) and low energy consumption (allowing portability). Charge transfer between nanotubes and adsorbed molecules could also cause drastic changes in the nanotubes' conductance, providing a chemical gating effect that could be utilized for molecular sensing [15]. However, most of these studies have focused on single-walled carbon nanotubes (SWNT), whereas on the other hand, multi-walled carbon nanotubes (MWNT) can be produced with relatively high purity (90%), are not subject to chirality restrictions on electrical properties, are less sensitive to damages resulting from chemical grafting, are generally amenable to more aggressive processing and can be produced with a lower price at a larger scale. This is why we have reported in this paper different ways to optimize the sensitivity and the selectivity of CNT-based quantum resistive sensors (QRS) for VOC analysis at room temperature, by controlling their conducting architecture's structure and chemical nature.

2. Experimental

2.1. Materials

All grades of MWNT were kindly provided by Nanocyl® (Sambreville, Belgium). These carbon nanotubes (CNT) are produced via a catalytic carbon vapor deposition (CCVD) process and according to thermogravimetric analysis TGA measurements from the producer. Carbon purity is 90% (10% catalyst) for CNT 7000 and short CNT, and higher than 95% (5% metal oxide) for NH_2, OH and COOH functionalized CNT. According to X-ray photoemission spectrometry (XPS) measurements from the producer, the functionalizations of CNT are respectively less than 0.5%, 6% and 4% for NH_2,

OH and COOH functionalized CNT. CNT were used without any further purification and dried under vacuum at 60 °C temperature for 24 h prior to solution preparation. Chloroform, methanol, tetrahydrofuran (THF) and toluene were obtained from Aldrich (Saint-Quentin Fallavier, France). All solvents were of analytical grades and used without any further purification. A description of the CNT characteristics is given in Table 1. Conductive polymer nanocomposite (CPC) solutions were obtained by dispersing CNT in the following polymer matrices: LEXAN141R poly(carbonate) (PC) purchased from GE Plastics (Belfort, France), poly(methyl methacrylate) (PMMA) VQ 101S purchased from Rohm (Emmerich am Rhein, Germany) and flakes of atactic poly(styrene) (aPS) purchased from Polyscience (Paris, France) with an average molar mass of M_n = 50,000 g·mol^{-1}.

Table 1. Carbon nanotube (CNT) characteristics. XPS, X-ray photoemission spectrometry.

Property	Value					Technique
	7000	**short**	**NH_2**	**OH**	**COOH**	
Average Diameter	9.5 nm	9.5 nm	9.5 nm	9.5 nm	9.5 nm	TEM
Average Length	1.5 µm	<1 µm	<1 µm	<1 µm	<1 µm	TEM
Carbon Purity	90%	90%	>95%	>5%	>95%	TGA
Metal Oxide (impurity)	10%	10%	<5%	<5%	<5%	TGA
Functionalization			<0.5%	<6%	<4%	XPS

2.2. Techniques

2.2.1. Fabrication of CNT Transducers by Spraying Layer-by-Layer (sLbL)

To obtain a good dispersion and homogeneous solutions, CNT were introduced into chloroform and dispersed under sonication with a Branson 3510 device (100 W, 40 kHz) for 6 h at 60 °C (in a temperature controlled bath). Typically, 6 mg of CNT were dispersed in 20 cm^3 of liquid chloroform. In the second step, the spray deposition was done layer-by-layer [40] to form a thin CNT random network onto homemade interdigitated microelectrodes (IDE). IDE were prepared by a cross-section cut of commercial 22 nF ceramic capacitors, which leads to interdigitated metal lines (25% Ag/75% Pd), separated by 15 µm. After cutting, electrodes were polished unidirectionally and washed with ethanol to remove any remaining particles. After being sprayed, samples were dried at 30 °C for one night. Spraying was done using a homemade device, allowing for the precise control of the spraying conditions, such as the nozzle flow rate, the air pressure, the sweep speed and the target to nozzle distance. In order to have transducers whose sensitivity will not change due to variations in their thickness, the previous parameters and the number of sprayed layers were kept constant for all the samples during the sensing experiments (Figure 1).

2.2.2. Fabrication of CPC Transducers by sLbL

The same kind of procedure as for neat CNT transducers was used to fabricate conductive polymer nanocomposite (CPC) transducers. Only the following conditions of fabrication of the solution by spraying were changed. Polymers were first dissolved in chloroform, and then, 1% of CNT (percentage relatively to the polymer mass) was added. The concentration of polymer-CNT in the solution was 10 g·dm^{-3}. CPC solutions were homogenized by sonication for 90 min at 25 °C and

further degassed for 5 min. Optimal spray conditions were obtained with a nozzle scanning speed of V_s = 10 cm s^{-1}, a solution flow rate on index 2, a stream pressure of p_s = 0.20 MPa and a target to nozzle distance of d_{tn} = 8 cm. After solvent evaporation, the welding of CPC microdroplets of 15 to 60 µm forms a hierarchical 3D percolated network [41]. Each sprayed layer is about 35 to 40 nm-thick. In this study, all CPC transducers were composed of 5 sprayed layers.

Figure 1. Comparison of the CNT random network transducers' response to methanol vapor depending on their form, *i.e.*, 5-layer film sprayed layer-by-layer (**top**) or bucky paper made under vacuum (**bottom**). sLbL, sprayed layer-by-layer.

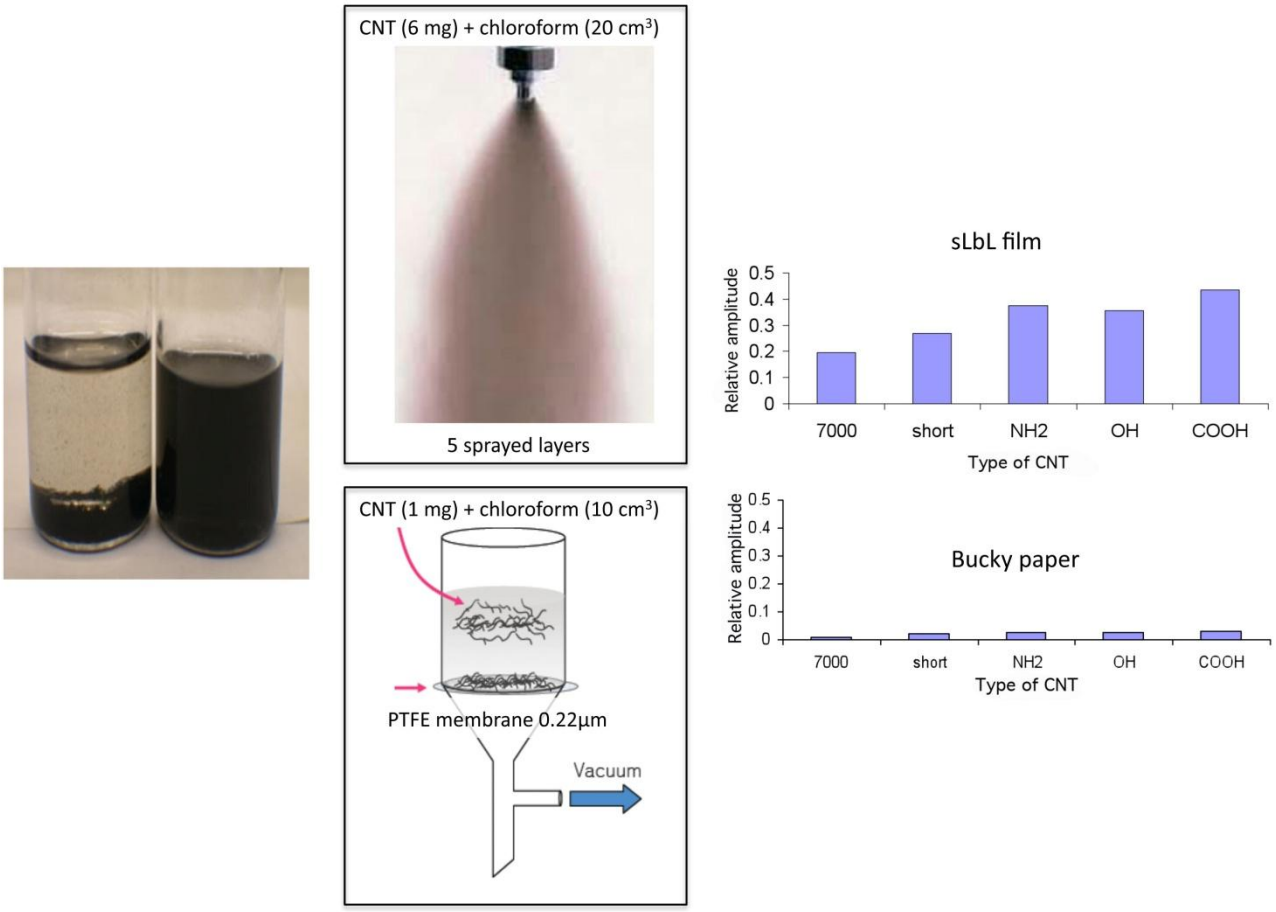

2.2.3. Fabrication of CNT Transducers by Filtration on a PTFE Membrane under Vacuum to Make Bucky Papers (BP)

For the fabrication of bucky paper (BP) transducers [42], the first step of the dispersion of CNT in solution under sonication was analogous to that previously described for sLbL processing. Typically, 1 mg of CNT was introduced in 10 cm^3 of liquid chloroform. Then, the solution was poured onto a 0.22 µm porous diameter, poly(tetrafluoroethelene) PTFE filtration membrane and filtrated under vacuum. The BP transducer was then dried at 30 ℃ for one night. The freestanding BP transducer was peeled off the membrane after the drying process was complete and deposited on IDE for further vapor sensing experiments (Figure 1).

2.2.4. Atomic Force Microscopy Characterization (AFM)

The nanoscale morphology of CNT sensors was investigated by atomic force microscopy in ambient conditions using the light tapping mode (TM-AFM) on a Nanoscope IIIa multimode scanning probe microscope from Digital Instruments-Veeco (Paris, France). The ratio of the set point amplitude to the free amplitude was maintained at 0.9 and RTESP tips from Veeco, with typical resonance frequency between 300 and 400 kHz, and a radius between 5 and 15 nm was used. CNT solution was sprayed on mica instead of microelectrodes to decrease the surface roughness below the micron and to obtain nice AFM pictures. The conditions of spraying were the same as for CNT sensor fabrication.

2.2.5. Dynamical Vapor Sensing Measurement

Gas sensing properties were investigated by recording the CNT electrical responses upon exposure to alternative 10-min cycles of nitrogen (N_2) and solvent vapors. The dynamic system consisting of mass flow controllers, solvent bubblers and electrical valves is controlled by LabView software. Bubbling N_2 gas in liquid solvent provides a saturated vapor stream, which was, in turn, diluted by a second N_2 flow to the desired concentration at room temperature. The design of the device allows one to keep constant the total flow rate at Qv = 100 $cm^3 \cdot min^{-1}$, while the analytic flow rate is set to Qv = 10 $cm^3 \cdot min^{-1}$, 50 $cm^3 \cdot min^{-1}$ or 100 $cm^3 \cdot min^{-1}$ to investigate the effect of the analytic flow rate. The mass flow controllers used were EL-FLOW from Bronkhorst. The electrical characteristics of the CNT transducer were recorded with a Keithley 6517A multimeter [43]. Samples were placed in a 9 × 3 × 3.5 cm^3 chamber with 6 slots. A description of the experimental device is given in Figure 2.

Figure 2. Scheme of the dynamic vapor sensing device, transducers and typical responses of CNT 7000 (**left**) and functionalized CNT (**right**) to chloroform vapor pulses.

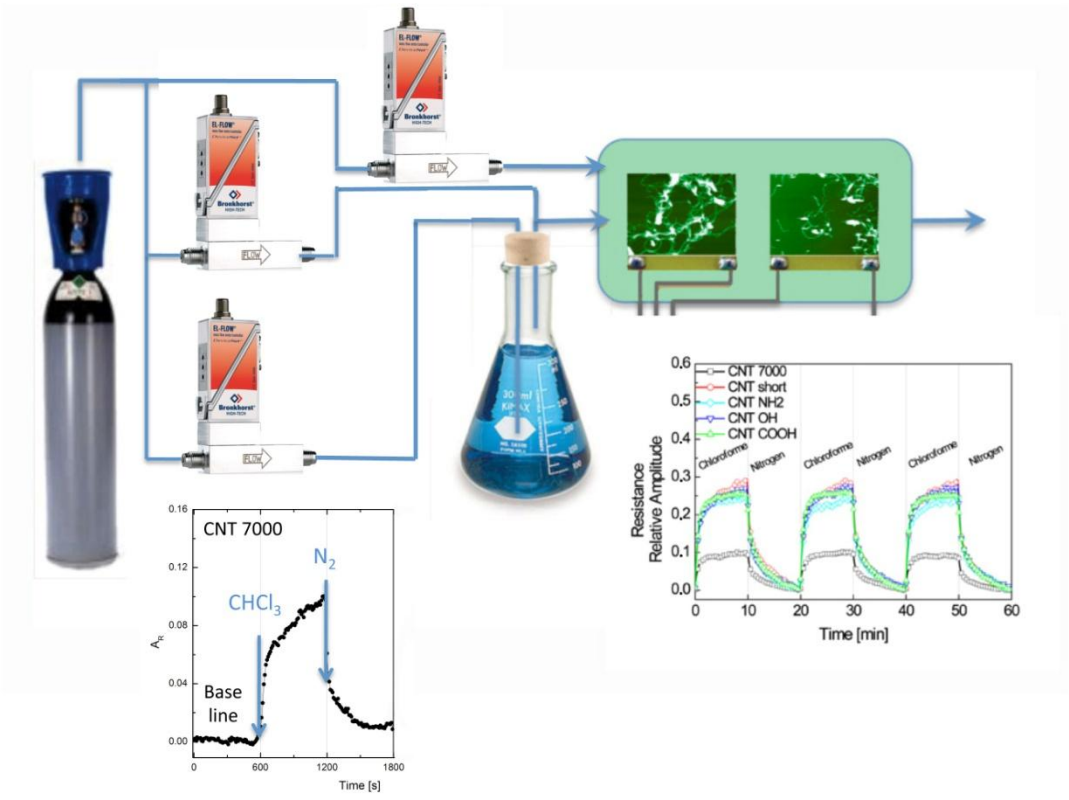

2.2.6. Data Analysis Using Principal Component Analysis (PCA)

There are several algorithms available for chemical sensing data analysis, but one of the most popular is Principal Component Analysis (PCA) [44–46]. PCA is a powerful tool for pattern recognition, by which the multivariate datasets have been transformed into a coordinate space. The vectors in this new coordinate set are the principal components (PC) of the data stream; accordingly, the VOC can be separated and projected onto this map. In fact, the dataset obtained from e-noses is mostly processed by the PCA method, which is frequently used for the anticipated diagnosis of diseases [47–50]. In this study, the data from four sensors (CNT short, functionalized by COOC, OH and NH_2), assembled into an array constituting an e-nose, were analyzed by using the PCA treatment implemented in the TANAGRA software [51].

3. Results and Discussion

3.1. Selection of Transducers' Optimal Process

Figure 1 summarizes different elements useful for comparing the two processes selected for the fabrication of CNT transducers already presented in the technical part: spraying layer-by-layer and filtration under vacuum. Firstly, it is obvious that the BP technique is the simplest, as it requires a limited amount of equipment. However, in practice, this technique leads to CNT random networks, whose density and thickness are generally too high to really benefit from tunneling conduction, operating in more easily disconnectable networks. Moreover, the decrease of conductivity of such transducers will yield thin films that are very difficult to handle without breakage. On the contrary, the sLbL process is found to be much more versatile for the preparation of CNT transducers for VOC sensing, as it allows one to adjust the random network density by acting on both the formulation of the spray solution and on the number of sprayed layers. Consequently, sLbL of only five layers provides transducers with larger chemoresistive responses than BP, whatever the CNT shape (long or short) and functionality (NH_2, OH or COOH), as evidenced in Figure 1 (inset). This is the reason why sLbL has been selected for the fabrication of all other sensors studied in the present paper.

3.2. Analysis of Transducer's Morphology by AFM

The architecture of CNT random networks has been investigated by AFM for 7000 and short CNT. Samples were prepared by spraying five layers of a CNT solution in chloroform onto freshly cleaved mica substrates. Typical AFM images (Figure 3) illustrate the random nature of the conducting network morphology of the two kinds of CNT well. The high magnification (2×2 μm^2 full scale), allows for differentiating the two types of CNT, long and short, in the network well. In agreement with the characteristics given by the producer, CNT 7000 have a length comprising between 0.8 µm and 1 µm and a diameter between 50 and 100 µm, whereas short CNT length is comprised between 0.5 and 0.8 µm, with about the same diameter as CNT 7000. AFM pictures show that the CNT 7000 network is denser than that of short CNT. The fact that CNT 7000 are longer also explains their more important ability to make entanglements. All functionalized CNT random networks have similar morphologies to that of short CNT and, thus, will not be presented. An optimal morphology for CNT

random networks dedicated to vapor sensing is expected to exhibit a large specific surface able to adsorb a maximum of target molecules, which will easily disconnect CNT/CNT junctions upon local solvation.

Figure 3. Atomic force microscopy (AFM) pictures (2 µm full scale) showing the morphology of the two sprayed layer-by-layer (LbL) CNT random networks as a function of CNT length: (**left**) CNT 7000; (**right**) CNT short (the images are also present in Figure 2).

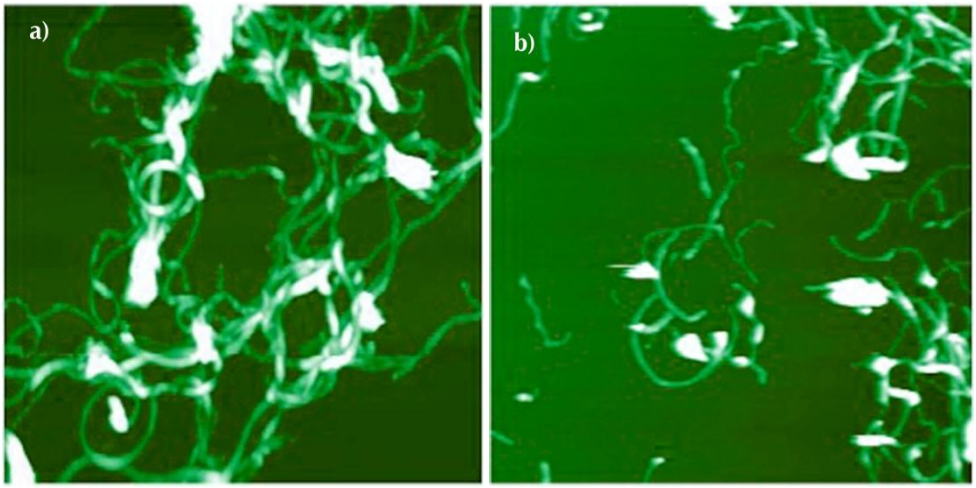

3.3. Vapor Sensing Performances of Transducers

3.3.1. Chemoresistive Behavior

The vapor sensing ability of QRS finds its origin in the perturbation of electrons' motion in the CNT random network due to the variations of the CNT/CNT junctions' gaps. Any disconnection of the network tends to promote tunneling conduction (decreasing exponentially with the gap) to the detriment of ohmic conduction, which requires close contact between nanofillers. Consequently, the resistance of the sensors changes a lot with only a tiny amount of VOC molecules, for average gap variations not much more than 10 nm. As the local solvatation of CNT/CNT junctions depends on the interactions of the chemical functions present on the surface of CNT-polymers with those present on the analytes, the resulting variations in the gap will lead to differences in global resistance, thus allowing discrimination between them [52]. The best way to investigate the CNT network transducers' performances in terms of sensitivity and selectivity is to expose them to a set of vapors of different chemical natures, such as methanol, chloroform, THF and toluene, of decreasing polarities, as summarized in Table 2. The typical chemoresistive behavior of CNT sensors expressed by calculating their relative resistance amplitude with Equation (1), when exposed to pulses of a chloroform constant flow rate of 100 $cm^3 \cdot min^{-1}$, is well illustrated in Figure 2 (inset).

$$A_r = \frac{R - R_0}{R_0} \quad (1)$$

where R and R_0 are, respectively, the CNT sensors' resistance in the presence of vapor and the initial resistance in dry N_2 flow.

Typically, CNT sensors exhibit a positive vapor coefficient (PVC), *i.e.*, solvent molecules decrease the intensity of the current in the transducer, resulting in a positive variation of resistance. A good sensor is expected to have a quick electrical response with a large and reproducible amplitude. The shape of the different responses shows that upon exposure to solvent vapors, CNT sensors reach their maximum amplitude within a couple of minutes. In the second part of the cycle, during the desorption step, when transducers are exposed to a dry nitrogen flow, the relative resistance's amplitude decreases quite instantaneously by about 50%, then slower, to reach its initial value at 10 min. Figure 4 shows the responses of CNT sensors for methanol, chloroform, **tetrahydrofuran** (THF) and toluene. The same features are observed for all the vapors, *i.e.*, all systems are thermodynamically stable, reach saturation quickly, but lead to a reversible signal that suggests the complete desorption of the analytes. As expected of selective transducers, the amplitude of their response changes with the nature of the VOC, which allows their ranking. The first striking feature is that all CNT sensors have sensitivities increasing according to the polarity of the target molecules. Secondly, the sensitivity of CNT sensors depends on their functionality as follows: COOH, NH_2, OH, short and long (7000); this trend being more or less visible depending on the vapor's polarity.

Table 2. Solvent characteristics.

	Polarity Constant (N)	Molar mass *(g mol^{-1})*	Density at 20 °C *(g cm^{-3})*
Methanol CH_4O	0.762	32.04	0.7910
Chloroform $CHCl_3$	0.259	119.38	1.4891
THF C_4H_8O	0.207	72.11	0.8892
Toluene C_7H_8	0.099	92.14	0.8668

Figure 4. Responses of CNT sensors to methanol, chloroform, THF and toluene (standard set of volatile organic compounds (VOC)).

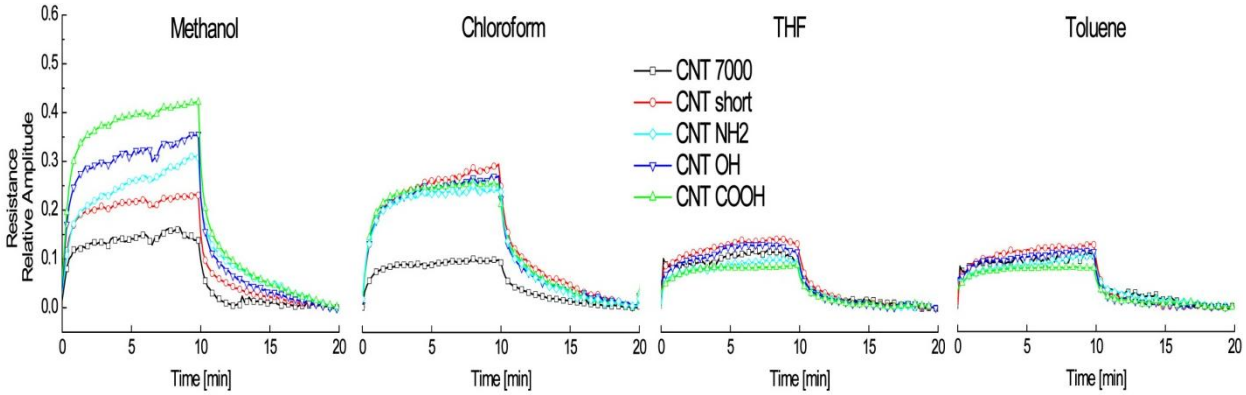

3.3.2. Quantitativity of Sensors' Responses

To investigate the relationship between the response amplitude and the amount of analyte molecules impacting on the sensor per minute, the volume flow rate (Q_v) was increased from Q_v = 10 cm^3 min^{-1} to Q_v = 50 cm^3 min^{-1} and, finally, to Q_v =100 cm^3 min^{-1}. Figure 5 summarizes the

different responses recorded for CNT sensors exposed to pulses of methanol and chloroform vapors, using 10, 50 and 100 cm^3 min^{-1} flow rates. It can be seen that the amplitude of their relative resistance grows almost linearly with an increasing flow rate and does so whatever the CNT and solvent types, which makes it useless to use the Langmuir-Henry-Clustering (LHC) model developed for non-linear systems [32,33,43]. Moreover, the response growth depends on the vapors' nature, and thus, the slopes of the corresponding curves are different, and this provides another way to distinguish VOC. Additionally, it can be noted that increasing the vapor flow rate is equivalent to an increase of vapor concentration, even if this parameter is kept constant initially.

Figure 5. Quantitativity of the signals of the CNT sensors when exposed to methanol (**left**) and chloroform (**right**) at different vapor flow rates (the effects of the amount of molecules).

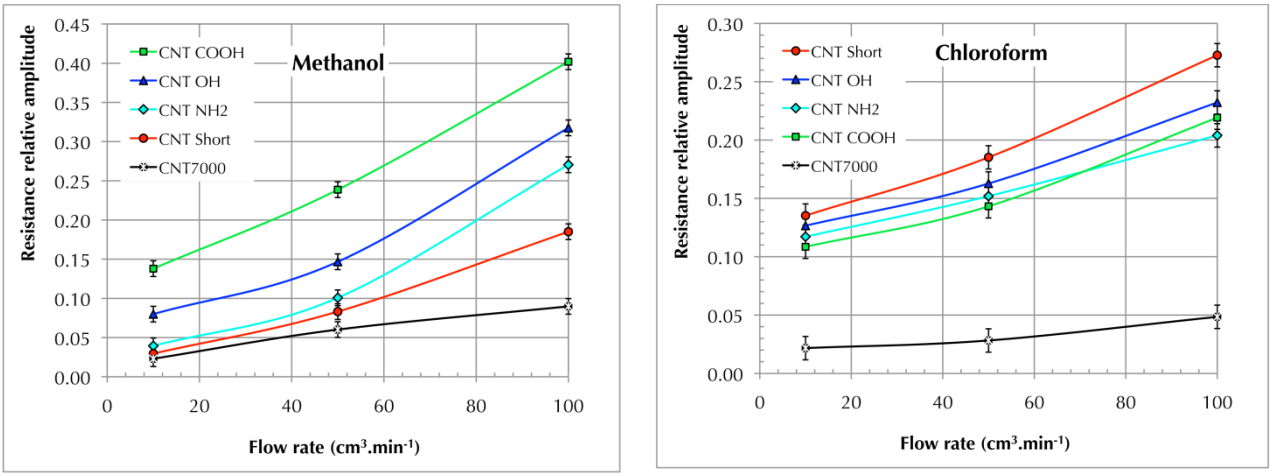

3.3.3. Vapor Discrimination Ability of CNT Sensors

Figure 6(left) summarizes in a single graph all the responses' maxima for the five CNT-based sensors exposed to the four selected vapors, methanol, chloroform, THF and toluene. It appears now more clearly than in Figure 4 that every sensor/analyte couple has a distinct chemoresistive imprint suitable for VOC discrimination. This is also highlighted by Figure 6(right), which presents the PC1–PC2 map for an array of four sensors successively exposed to the four selected VOC after PCA data processing. All the vapors have been successfully classified into four groups on the basis of the nature of the vapor, *i.e.*, polarity, chemical nature, *etc.* These results demonstrate the perfect adequacy of the selected set of CNT sensors for effective VOC discrimination. This is because the long CNT (CNT 7000) network is denser than the short CNT one. CNT sensor selectivity can be deduced from these parameters and can lead to a different ranking than that suggested by Figure 4. If used as an e-nose, this array should be able to identify unknown chemical species, by recording electrical signals and processing data via a pattern recognition algorithm, such as Principal Component Analysis.

Figure 6. Selectivity of CNT sensors towards methanol, chloroform, THF and toluene expressed directly in bar graph (**left**) and after Principal Component Analysis (PCA) treatment of the data from an e-nose (**right**).

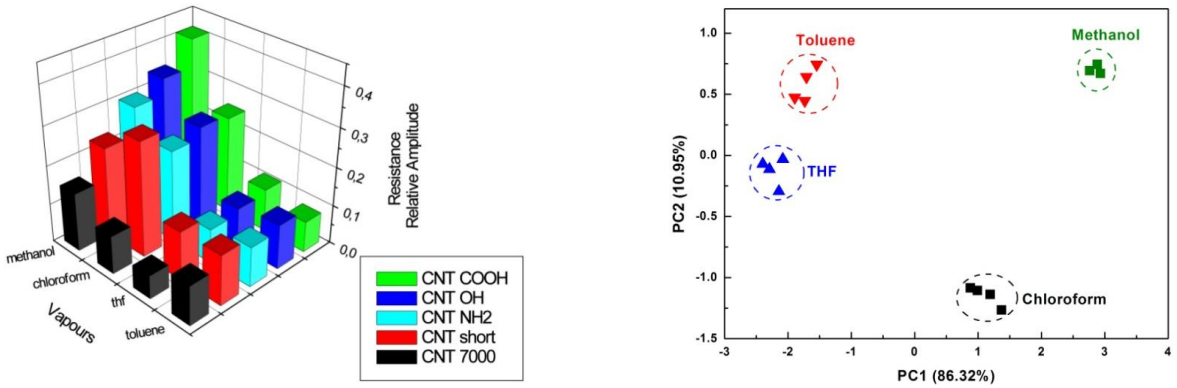

3.3.4. Input of Polymer Matrices in the Sensitivity and Selectivity of Sensors

The first striking feature highlighted by the comparison between Figure 7(left and right), which summarizes the chemoresistive responses of CPC sensors synthesized by combining three types of polymer matrices (PS, PMMA and PC) with two kinds of CNT (neat CNT 7000 and COOH functionalized CNT) is that COOH functionalized CNT tend to strongly decrease the transducers' sensitivity compared to 7000 CNT. It is particularly visible with the response of PC-1%-CNT 7000 to chloroform, which reaches almost 25, whereas that of PC-1%-CNT COOH is only about 0.4. The second important trend is that the association of CNT with polymers strongly increases the sensors' response amplitude compared to simple CNT functionalization (see Figure 6(right)). Thus, the simple adsorption of polymers on CNT appears much more effective than their chemical grafting, to enhance the transducers' selectivity and sensitivity. This route has also been explored in another work investigating the importance of the ways of bringing the polymer to the CNT/CNT junctions and the effect of the polymer/CNT ratio on the CPC transducers' sensitivity [53]. Additionally, it can be noticed in Figure 7 that although CNT grafting decreases the amplitude of the responses, it does not affect their ranking much, *i.e.*, their selectivity.

Figure 7. The influence of both the polymer matrix (poly(styrene) (PS), poly(methyl methacrylate) (PMMA) and poly(carbonate) (PC)) and CNT treatment on the sensors' chemoresistive responses when conductive polymer nanocomposite (CPC) are filled with (**left**) neat 7000 CNT and (**right**) COOH functionalized CNT.

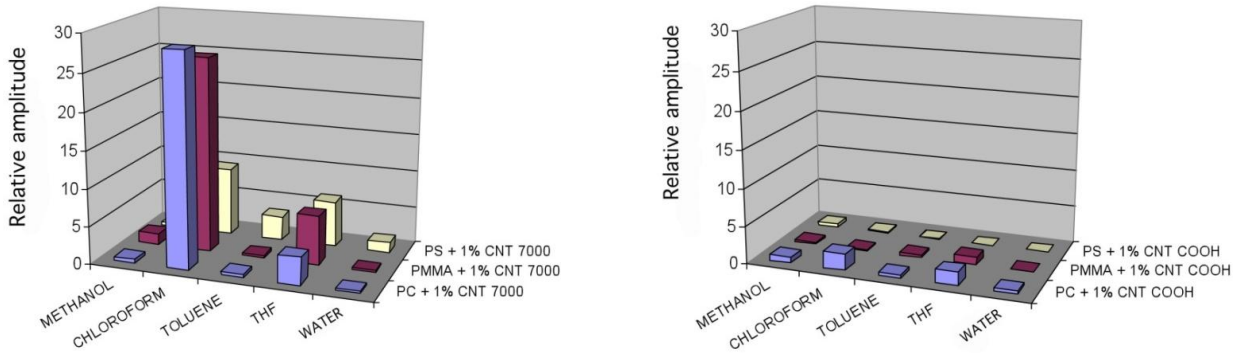

4. Conclusions

We have developed a simple, reliable and reproducible CNT sensor platform for volatile organic compound (VOC) analysis at room temperature. The CNT sensors' chemoresistive behavior has been investigated by submitting them to sequential pulses of saturated vapors, such as methanol, chloroform, toluene and THF. The results further indicate that both the selectivity and sensitivity of the transducers can be improved through several mechanisms that optimize the CNT network structure or enhance the interactions between VOC and carbon nanotubes. To optimize the conducting architecture, the spraying layer-by-layer process was found to be superior to filtration under vacuum (bucky paper), whereas non-covalent bonding of polymer chains led to a more effective disconnection of CNT/CNT junctions than chemical grafting, upon specific molecular interactions with VOC. These results demonstrate the perfect adequacy of the selected set of CNT sensors, to rank different VOC by polarity. Moreover, the PCA analysis showed that CNT sensors are good candidates for a further implementation into an array (e-nose) for VOC identification. Finally, Figure 8 illustrates the promising applications of CNT-based chemoresistive sensors, in safety and heath fields, such as environmental sensing [54], smart packaging [55,56] and anticipated disease diagnosis [47–50]. In fact, either the VOC produced by the combustion of fuels (outdoor) or those released by cleaning products or materials (indoor) are being found at amounts close to the limit of exposure over which they become dangerous for health. Conversely, the production of VOC biomarkers by either specific bacteria or cancerous cells is providing a fantastic opportunity to improve human health. There is thus a need to develop low-cost VOC sensors that can be widely implemented in portable devices with low energy consumption. We expect that CNT-based QRS will be good candidates for such applications, provided that some issues are resolved, such as the persistence of their selectivity at ultra-low VOC concentrations (ppb level) and during exposure to complex blends of similar VOC.

Figure 8. Different kinds of applications of CNT-based arrays of sensors (e-nose). (**Left**) Environmental monitoring to evaluate the level of exposition to toxic VOC for humans; (**right**) analysis of VOC biomarkers of food degradation (meat, fruits, *etc.*) and disease development (lung cancer, diabetes *etc.*).

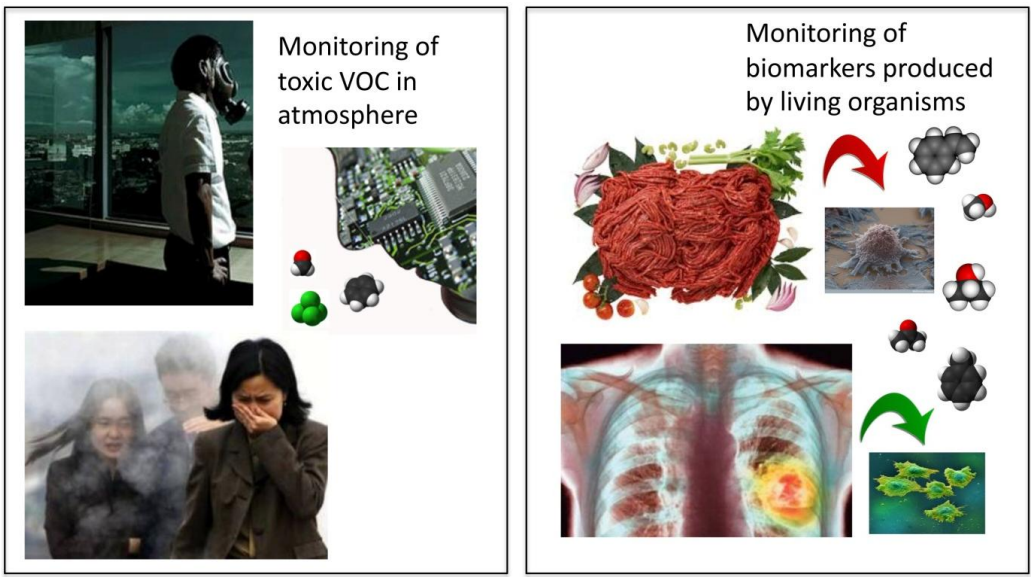

Acknowledgments

The authors are grateful to Hervé Bélégou, Isabelle Pillin and Frédéric Luizi for their contribution to this work. This research was funded by INTELTEX (intelligent multi-reactive textiles integrating nanofiller-based CPC-fibers), a European Integrated Project supported by the Sixth Framework Program for Research and Technological Development of the European Commission (NMP2-CT-2006-026626).

Conflicts of Interest

The authors declare no conflict of interest.

References

1. Radushkevich, L.V.; Lukyanovich, M.V. About the structure of carbon formed by thermal decomposition of carbon monoxide on iron substrate. *J. Phys. Chem.* (Moscow) **1952**, *26*, 88–95.
2. Iijima, S. Helical microtubules of graphitic carbon. *Nature* **1991**, *354*, 56–58.
3. Dillon, A.C.; Gilbert, K.E.H.; Parilla, P.A.; Alleman, J.L.; Hornyak, G.L.; Jones, K.M.; Heben, M.J. Storage of hydrogen in single-walled carbon nanotubes. *Nature* **1997**, *386*, 377–379.
4. Chambers, A.; Park, C.; Baker, R.T.K.; Rodriguez, N.M. Hydrogen storage in graphite nanofibers. *J. Phys. Chem. B* **1998**, *102*, 4253–4256.
5. Ahn, C.C.; Ye, Y.; Ratnakumar, B.V.; Witham, C.; Bowman, R.C.; Fultz, B. Hydrogen desorption and adsorption measurements on graphite nanofibers. *Appl. Phys. Lett.* **1998**, *73*, 3378–3381.
6. Flujiwara, A.; Ishii, K.; Suematsu, H.; Kataura, H.; Maniwa, Y.; Suzuki, S.; Achiba, Y. Gas adsorption in the inside and outside of single-walled carbon nanotubes. *Chem. Phys. Lett.* **2001**, *336*, 205–211.
7. Collins, P.G.; Bradley, K.; Ishigami, M.; Zettle, A. Extreme oxygen sensitivity of electronic properties of carbon nanotubes. *Science* **2000**, *287*, 1801–1804.
8. Sumanasekera, G.U.; Adu, C.K.W.; Fang, F.; Eklund, P.C. Effect of gas adsorption on electrical transport in single walled carbon nanotubes. *Phys. Rev. Lett.* **2000**, *85*, 1096–1099.
9. Zahab, A.; Spin, L.; Poncharaal, P. Water vapour effect on the electrical conductivity of a single walled carbon nanotube mat. *Phys. Rev. B* **2000**, *62*, 10000–10003.
10. Zhao, J.; Buldum, A.; Han, J.; Lu, J.P. Gas molecule adsorption in carbon nanotubes and nanotube bundles. *Nanotechnology* **2002**, *13*, 195–200.
11. Chang, H.; Lee, J.D.; Lee, S.M.; Lee, Y.H. Adsorption of NH_3 and NO_2 molecules on carbon nanotubes. *Appl. Phys. Lett.* **2001**, *79*, 3863–3866.
12. Cantalini, C.; Valentini, L.; Armentano, I.; Lozzi, L.; Kenny, J.M.; Santucci, S. Sensitivity to NO_2 and cross-sensitivity analysis to NH_3, ethanol and humidity of carbon nanotubes thin film prepared by PECVD. *Sens. Actuators B: Chem.* **2003**, *95*, 195–202.
13. Kong, J.; Franklin, N.R.; Zhou, C.; Chapline, M.; Peng, S.; Cho, K.; Dai, H. Nanotubes molecular wires as chemical sensors. *Science* **2000**, *287*, 622–625.
14. Adu, C.K.W.; Sumanasekera, G.U.; Pradhan, B.K.; Romero, H.E.; Eklund, P.C. Carbon nanotubes: A thermoelectric nano-nose. *Chem. Phys. Lett.* **2001**, *337*, 31–35.

15. Dai, H. Carbon nanotubes: Synthesis, integration, and properties. *Acc. Chem. Res.* **2002**, *35*, 1035–1044.
16. Li, J.; Lu, Y.; Ye, Q.; Cinke, M.; Han, J.; Meyyappan, M. Carbon nanotube sensors for gas and organic vapor detection. *Nano Lett.* **2003**, *3*, 927–933.
17. Someya, T.; Small, J.; Kim, P.; Nuckolls, C.; Yardley, J.T. Alcohol vapor sensors based on single-walled carbon nanotube field effect transistors. *Nano Lett.* **2003**, *3*, 877–881.
18. Kauffman, D.R.; Star, A. Carbon nanotube gas and vapor sensors. *Angew. Chem. (Int. Ed.)* **2008**, *47*, 6550–6570.
19. Goldoni, A.; Petaccia, L.; Lizzit, S.; Larciprete, R. Sensing gases with carbon nanotubes: A review of the actual situation. *J. Phys.: Condens. Matter* **2010**, *22*, 1–8.
20. Madu, M.J.; Morrison, S.R. *Chemical Sensing with Solid State Devices*; Academic Press: New York, NY, USA, 1989.
21. Seiyama, T. *Chemical Sensors-Current State and Future Outlook: Chemical Sensor Technology*; Kodansha & Elsevier: Amsterdam, The Netherlands, 1988.
22. Arshak, K.; Gaidan, I. Development of a novel gas sensor based on oxide thick films. *Mater. Sci. Eng. B* **2005**, *118*, 44–49.
23. Wang, J.X.; Sun, X.W.; Yang, Y.; Huang, H.; Lee, Y.C.; Tan, O.K.; Vayssieres, L. Hydrothermally grown oriented ZnO nanorod arrays for gas sensing applications. *Nanotechnology* **2006**, *17*, 4995–4998.
24. Belchi, A.d.; Rothpfeffer, N.; Pelegrí-Sebastia, J.; Chilo, J.; Rodriguez, D.G.; Sogorb, T. Sensor characterization for multisensor odor discrimination system. *Sens. Actuators B: Chem.* **2013**, *191*, 68–72.
25. Hirsch, A. Functionalization of single-walled carbon nanotubes. *Angew. Chem. (Int. Ed.)* **2002**, *41*, 1853–1859.
26. Bahr, J.L.; Tour, J.M. Covalent chemistry of single-wall carbon nanotubes. *J. Mater. Chem.* **2002**, *12*, 1952–1958.
27. Kong, L.; Wang, J.; Fu, X.; Zhong, Y.; Meng, F.; Luo, T.; Liu, J. p-Hexafluoroisopropanol phenyl covalently functionalized single-walled carbon nanotubes for detection of nerve agents. *Carbon* **2010**, *48*, 1262–1270.
28. Castro, M.; Lu, J.; Bruzaud, S.; Kumar, B.; Feller, J.F. Carbon nanotubes/poly(e-caprolactone) composite vapour sensors. *Carbon* **2009**, *47*, 1930–1942.
29. Lou, X.; Daussin, R.; Cuenot, S.; Duwez, A.S.; Pagnoulle, C.; Detrembleur, C.; Bailly, C.; Jérôme, R. Synthesis of pyrene-containing polymers and noncovalent sidewall functionalization of multiwalled carbon nanotubes. *Chem. Mater.* **2004**, *16*, 4005–4011.
30. Zhao, Y.L.; Stoddart, J.F. Noncovalent functionalization of single-walled carbon nanotubes. *Acc. Chem. Res.* **2009**, *42*, 1161–1171.
31. Shim, M.; Kam, N.W.S.; Chen, R.J.; Li, Y.; Dai, H. Functionalization of carbon nanotubes for biocompatibility and biomolecular recognition. *Nano Lett.* **2002**, *2*, 285–288.
32. Feller, J.F.; Kumar, B.; Castro, M. Conductive Biopolymer Nanocomposites for Sensors. In *Nanocomposites with Biodegradable Polymers: Synthesis, Properties & Future Perspectives*, 1st ed.; Mital, V., Ed.; Oxford University Press: Oxford, UK, 2011; pp. 368–399.

33. Kumar, B.; Park, Y.T.; Castro, M.; Grunlan, J.C.; Feller, J.F. Fine control of carbon nanotubes—Polyelectrolyte sensors sensitivity by electrostatic layer by layer assembly (eLbL) for the detection of volatile organic compounds (VOC). *Talanta* **2012**, *88*, 396–402.
34. Zanolli, Z.; Leghrib, R.; Felten, A.; Pireaux, J.J.; Llobet, E.; Charlier, J.C. Gas sensing with Au-decorated carbon nanotubes. *ACS Nano* **2011**, *5*, 4592–4599.
35. Yoon, H.; Xie, J.; Abraham, J.K.; Varadan, V.K.; Ruffin, P.B. Passive wireless sensors using electrical transition of carbon nanotube junctions in polymer matrix. *Smart Mater. Struct.* **2006**, *15*, S14–S20.
36. Mabrook, M.F.; Pearson, C.; Jombert, A.S.; Zeze, D.A.; Petty, M.C. The morphology, electrical conductivity and vapour sensing ability of inkjet printed thin films of single-wall carbon nanotubes. *Carbon* **2009**, *47*, 752–757.
37. Bondavalli, P.; Legagneux, P.; Pribat, D. Carbon nanotubes based transistors as gas sensors: State of the art and critical review. *Sens. Actuators B: Chem.* **2009**, *140*, 304–318.
38. Kumar, B.; Castro, M.; Feller, J.F. Tailoring the chemo-resistive response of self-assembled polysaccharide-CNT sensors by chain conformation at tunnel junction. *Carbon* **2012**, *50*, 3627–3634.
39. Kumar, B.; Castro, M.; Feller, J.F. Controlled conductive junction gap for chitosan—Carbon nanotubes quantum resistive vapour sensors. *J. Mater. Chem.* **2012**, *22*, 10656–10664.
40. Feller, J.F.; Grohens, Y. Electrical response of poly(styrene)/carbon black conductive polymer composites (CPC) to methanol, toluene, chloroform and styrene vapors as a function of filler nature and matrix tacticity. *Synth. Metals* **2005**, *154*, 193–196.
41. Robert, C.; Feller, J.F.; Castro, M. Sensing skin for strain monitoring made of PC-CNT Conductive Polymer Nanocomposite sprayed layer by layer. *ACS Appl. Mater. Interfaces* **2012**, *4*, 3508–3516.
42. Rein, M.D.; Breuer, O.; Wagner, H.D. Sensors and sensitivity: Carbon nanotube buckypaper films as strain sensing devices. *Compos. Sci. Technol.* **2011**, *71*, 373–381.
43. Feller, J.F.; Lu, J.; Zhang, K.; Kumar, B.; Castro, M.; Gatt, N.; Choi, H.J. Novel architecture of carbon nanotube decorated poly(methyl methacrylate) microbead vapour sensors assembled by spray layer by layer. *J. Mater. Chem.* **2011**, *21*, 4142–4149.
44. Hierlemann, A.; Gutierrez-Osuna, R. Higher-order chemical sensing. *Chem. Rev.* **2008**, *108*, 563–613.
45. Castro, M.; Kumar, B.; Feller, J.F.; Haddi, Z.; Amari, A.; Bouchikhi, B. Novel e-nose for the discrimination of volatile organic biomarkers with an array of carbon nanotube (CNT) conductive polymer nanocomposite (CPC) sensors. *Sens. Actuators B: Chem.* **2011**, *159*, 213–219.
46. Cole, M.; Covington, J.A.; Gardner, J.W. Combined electronic nose and tongue for a flavour sensing system. *Sens. Actuators B: Chem.* **2011**, *156*, 832–839.
47. D'Amico, A.; Pennazza, G.; Santonico, M.; Martinelli, E.; Roscioni, C.; Galluccio, G.; Paolesse, R.; Natale, C.D. An investigation on electronic nose diagnosis of lung cancer. *Lung Cancer* **2010**, *68*, 170–176.
48. Arasaradnam, R.P.; Quraishi, N.; Kyrou, I.; Nwokolo, C.U.; Joseph, M.; Kumar, S.; Bardhan, K.D.; Covington, J.A. Insights into "fermentonomics": Evaluation of volatile organic compounds (VOC) in human disease using an electronic "e-nose". *J. Med. Eng. Technol.* **2011**, *35*, 87–91.

49. Tisch, U.; Aluf, Y.; Ionescu, R.; Nakhleh, M.; Bassal, R.; Axelrod, N.; Robertman, D.; Tessler, Y.; Finberg, J.P.M.; Haick, H. Detection of asymptomatic nigrostriatal dopaminergic lesion in rats by exhaled air analysis using carbon nanotube sensors. *ACS Chem. Neurosci.* **2012**, *3*, 161–166.
50. Chatterjee, S.; Castro, M.; Feller, J.F. An e-nose made of carbon nanotube based quantum resistive sensors for the detection of eighteen polar/nonpolar VOC biomarkers of lung cancer. *J. Mater. Chem. B: Biol. Med.* **2013**, *1*, 4563–4575.
51. Rakotomalala, R. TANAGRA: Free software for teaching & Research. *EGC'2005 Proc.* **2005**, *2*, 697–702.
52. Lu, J.; Kumar, B.; Castro, M.; Feller, J.F. Vapour sensing with conductive polymer nanocomposites (CPC): Polycarbonate-carbon nanotubes transducers with hierarchical structure processed by spray layer by layer. *Sens. Actuators B: Chem.* **2009**, *140*, 451–460.
53. Kumar, B.; Castro, M.; Feller, J.F. Quantum resistive vapour sensors made of polymer coated carbon nanotubes random networks for biomarkers detection. *Chem. Sens.* **2013**, *3*, 1–7.
54. Nagle, H.T.; Gutierrez-Osuna, R.; Kermani, B.G.; Schiffman, S.S. *Chapter 22: Environmental Monitoring, Handbook of Machine Olfaction: Electronic Nose Technology*; Wiley VCH Verlag: Weinheim, Germany, 2002.
55. Ragazzo-Sanchez, J.A.; Chalier, P.; Chevalier, D.; Ghommidh, C. Electronic nose discrimination of aroma compounds in alcoholised solutions. *Sens. Actuators B: Chem.* **2006**, *114*, 665–673.
56. Peris, M.; Escuder-Gilabert, L. A 21st century technique for food control: Electronic noses. *Anal. Chim. Acta* **2009**, *638*, 1–15.